**Serial profiling of circulating tumor DNA identifies dynamic evolution of clinically actionable genomic alterations in high-risk neuroblastoma**

Kristopher R. Bosse[1,2]; Anna Maria Giudice[1]; Maria V. Lane[1]; Brendan McIntyre[1]; Patrick M. Schürch[1]; Guillem Pascual-Pasto[1]; Samantha N. Buongervino[1]; Sriyaa Suresh[1]; Alana Fitzsimmons[1]; Adam Hyman[1]; Maria Gemino-Borromeo[1]; Jennifer Saggio[1]; Esther R. Berko[1]; Alexander A. Daniels[1]; Jennifer Stundon[1]; Megan Friedrichsen[3]; Xin Liu[3]; Matthew L. Margolis[3]; Marilyn M. Li[4]; Marni Brisson Tierno[3]; Geoffrey R. Oxnard[3]; John M. Maris[1,2]; Yael P. Mossé[1,2]

[1]Division of Oncology and Center for Childhood Cancer Research, Children's Hospital of Philadelphia; Philadelphia, PA, 19104; USA

[2]Department of Pediatrics, Perelman School of Medicine at the University of Pennsylvania; Philadelphia, PA, 19104; USA

[3]Foundation Medicine, Inc. Cambridge, MA, 02141; USA

[4]Department of Pathology and Laboratory Medicine, Perelman School of Medicine at the University of Pennsylvania and the Children's Hospital of Philadelphia; Philadelphia, PA, 19104; USA

## Supplementary Methods

### Tumor sequencing

The CHOP Comprehensive NGS Solid Tumor Panel interrogates 238 cancer genes for sequence and copy number alterations (CNA) and 110 cancer genes for fusion genes as previously described (1-3). For sequence variant and CNA analysis, genomic DNA was extracted from the tumor samples. Libraries were prepared using custom-designed probes targeting the coding sequences, exon/intron boundaries, and selected promoter and intronic regions of the 238 genes (SureSelect, Agilent Technologies, Santa Clara, CA). For fusion analysis, target-specific primers covering 673 exons of the 110 genes were custom-designed to identify known or novel fusions using Anchored Multiplex PCR (AMP™) technology (ArcherDX, Inc. Boulder, CO). Total RNA (or total nucleic acid from FFPE samples) was extracted from the tumor samples and reverse-transcribed into cDNA. Libraries were constructed using ArcherTM Universal RNA Reagent Kit v2 for Illumina. Barcoded libraries were pooled and sequenced on the Illumina HiSeq platform using 150 bp paired-end sequencing (Illumina, San Diego, CA). DNA sequence data were analyzed using the homebrew software ConcordS v2 for SNVs/indels and NextGENe v2 NGS Analysis Software for CNAs (SoftGenetics, LLC, State College, PA). RNA sequence data were analyzed using Archer Analysis software and visualized with the JBrowse genome browser (Evolutionary Software Foundation, Berkeley, CA).

### *ERRFI1* expression profiling

*ERRFI1* mRNA expression data from neuroblastomas was accessed via the Genomics Analysis and Visualization Platform (R2; http://r2.amc.nl; Kocak; n = 649, SEQC; n = 498; and Westermann; n=579) (4-6).

**Event-free survival (EFS) analysis**

EFS analyses were performed utilizing the Kaplan Meier Scanner function in the Genomics Analysis and Visualization Platform (R2; http://r2.amc.nl; Kocak; n = 649, SEQC; n = 498; Cangelos; n=768; Oberthuer; n=251; and Westermann; n=144) (4-8).

**Supplementary Tables**

**Supplementary Table 1.** Summary of genes covered by the FoundationACT oligonucleotide baitset.

| GENES WITH COMPLETE EXON COVERAGE | | |
|---|---|---|
| **GENE** | **EXONS** | **AMPLIFICATIONS CALLED?*** |
| *BRCA1* | All exons | No |
| *BRCA2* | All exons | No |
| *CCND1* | All exons | Yes |
| *CD274* | All exons | Yes |
| *CDH1* | All exons | No |
| *CDK4* | All exons | Yes |
| *CDK6* | All exons | Yes |
| *CDKN2A* | All exons | No |
| *CRKL* | All exons | Yes (3 target regions) |
| *EGFR* | All exons | Yes |
| *ERBB2* | All exons | Yes |
| *ERRFI1* | All exons | No |
| *FGFR1* | All exons | Yes |
| *FGFR2* | All exons | Yes |
| *FOXL2* | All exons | No |
| *KRAS* | All exons | Yes |
| *MDM2* | All exons | Yes |
| *MET* | All exons | Yes |
| *MYC* | All exons | Yes (3 target regions) |
| *MYCN* | All exons | Yes |
| *NF1* | All exons | No |
| *PDCD1LG2* | All exons | Yes |
| *PTEN* | All exons | No |
| *PTPN11* | All exons | No |
| *SMO* | All exons | No |
| *TP53* | All exons | No |
| *VEGFA* | All exons | Yes |
| | | |
| **GENES WITH SELECT EXON COVERAGE** | | |
| **GENE** | **EXONS** | **AMPLIFICATIONS CALLED?** |
| *ABL1* | exon 4-9 | No |
| *AKT1* | exon 3 | No |
| *ALK* | exon 20-29 | Yes |
| *ARAF* | exon 4, 5, 7, 11, 13, 15, 16 | Yes |
| *BRAF* | exon 11-18 | Yes |
| *BTK* | exon 2, 15 | No |

| | | | |
|---|---|---|---|
| | *CTNNB1* | exon 3 | No |
| | *DDR2* | exon 5, 17, 18 | Yes (3 target regions) |
| | *ESR1* | exon 4-8 | Yes |
| | *EZH2* | exon 16 | No |
| | *FGFR3* | exon 7, 9, 14 | Yes (3 target regions) |
| | *FLT3* | exon 14, 15, 20 | Yes (3 target regions) |
| | *GNA11* | exon 4, 5 | No |
| | *GNAQ* | exon 4, 5 | No |
| | *GNAS* | exon 1 | No |
| | *HRAS* | exon 2, 3 | No |
| | *IDH1* | exon 4 | No |
| | *IDH2* | exon 4 | No |
| | *JAK2* | exon 14 | No |
| | *JAK3* | exon 5, 11, 12, 13, 15, 16 | No |
| | *KIT* | exon 8, 11, 12, 17 | Yes |
| | *MAP2K1* | exon 2, 3 | No |
| | *MAP2K2* | exon 2-4, 6, 7 | Yes |
| | *MPL* | exon 10 | No |
| | *MTOR* | exon 19, 30, 39, 40, 43-45, 47, 48, 53, 56 | Yes |
| | *MYD88* | exon 4 | No |
| | *NPM1* | exon 4-6, 8, 10 | No |
| | *NRAS* | exon 2, 3 | No |
| | *PDGFRA* | exon 18 | No |
| | *PDGFRB* | exon 12-21, 23 | Yes |
| | *PIK3CA* | exon 2, 3, 5-8, 10, 14, 19, 21 | Yes |
| | *RAF1* | exon 3, 4, 6, 7, 10, 14, 15, 17 | Yes |
| | *RET* | exon 11, 13-16 | Yes |
| | *TERT* | promoter | No |
| | | | |
| **GENES WITH SELECT INTRON COVERAGE** | | | |
| | **GENE** | **INTRONS** | |
| | *ALK* | intron 18, 19 | |
| | *EGFR* | intron 7 | |
| | *FGFR3* | intron 17 | |
| | *PDGFRA* | intron 7, 9 | |
| | *RET* | intron 9, 10, 11 | |
| | *ROS1* | intron 32, 33, 34 | |
| | | | |

***Amplifications are called for select genes.**
**Genes with ≥4 target regions are called; genes with three target regions are called and detected at lower sensitivity.**

**Supplementary Table 2.** Patient demographics and clinical covariates.

| | |
|---|---|
| **Patient characteristics** Number of patients (%) | **Sex**<br>24 (50%) Female<br>24 (50%) Male<br>**Age**<br>46 (96%) >18 months<br>2 (4%) <18 months<br>Median age 89.4 months<br>Range 0-405 months<br>**Disease status**<br>42 (88%) Relapse<br>4 (8%) New diagnosis<br>2 (4%) Disease progression<br>***MYCN* status**<br>33 (69%) Not amplified<br>12 (25%) Amplified<br>3 (6%) Unknown<br>**Samples/patient**<br>Total samples = 167<br>Median 3 samples/patient<br>Range 1-10 samples/patient<br>**ALK inhibitor therapy**<br>8 (17%) ceritinib<br>5 (10%) lorlatinib<br>1 (2%) alectinib<br>1 (2%) crizotinib |

**Supplementary Table 3.** Complete ctDNA profiling data - see excel sheet.

*Several *MYCN* “Novel rearrangements of unknown significance” are noted in column L of Supplementary Table 3 (denoted in italics) which could be related to the complex *MYCN* amplicon structure as previously reported (9,10).

**Supplementary Table 4.** ctDNA TP53 variant characteristics and associated clinical details.

| Patient # | Sample | # Variants | Variant (AA change) | Recent therapy | Days between therapy/ctDNA sequencing |
|---|---|---|---|---|---|
| **1** | A | 1 | **V143A** | $^{131}$I-MIBG | 46 |
| **3** | A | 4 | **E258D**<br>**G244C**<br>**T125M**<br>**G105C** | $^{131}$I-MIBG | 57 |
| **7** | B | 1 | **P151H** | HDM201 | 5 |
| **7** | C | 1 | **E271G** | $^{131}$I-MIBG | 117 |
| **7** | F,G | 1 | **P322fs*23** | $^{131}$I-MIBG | 36 |
| **13** | I | 3 | **A161T**<br>**C176F**<br>**R280S** | dinutuximab/ irinotecan/ temozolomide | 16 |
| **14** | A | 1 | **C135F** | nivolumab | 14 |
| **18** | B | 2 | **G279W**<br>**R248Q** | $^{131}$I-MIBG | 40 |
| **23** | A | 1 | **R158C** | crizotinib | 0 |
| **30** | B | 1 | **D281N** | $^{131}$I-MIBG | 41 |
| **38** | C | 3 | **R248Q**<br>**V218M**<br>**P177S** | $^{131}$I-MIBG | 53 |
| **41** | A-F | 1 | **V157fs*13** | Irino./Tem. | 17 |
| **41** | D-F | 1 | **G334V** | dinutuximab/ irinotecan/ temozolomide | 19 |
| **41** | F | 1 | **C277Y** | pazopanib | 0 |
| **48** | B | 2 | **P98S**<br>**splice site c.375+1G>A** | $^{131}$I-MIBG | 48 |

**Supplementary Table 5.** Summary of patients with ctDNA-tumor paired sequencing.

| Patient # | Disease status | ctDNA sequencing | Tumor sequencing (bolded genes not in ctDNA panel) | Tumor panel | Days between ctDNA/tumor sequencing | ctDNA/tumor discordance | ctDNA unique variants | Tumor sequencing supporting reads for ctDNA unique variants |
|---|---|---|---|---|---|---|---|---|
| **1** | Relapsed | *MYCN* amp., TP53 V143A | *MYCN* amp., ***RPTOR* amp.** | **FM** | **53** | **Yes** | TP53 V143A | No |
| **3** | Relapsed | ALK F1245V, *TERT* promoter -124C>T, TP53 E258D, TP53 G244C, TP53 T125M, TP53 G105C | ALK F1245V, *TERT* promoter -124C>T | **FM** | **63** | **Yes** | TP53 E258D, TP53 G244C, TP53 T125M, TP53 G105C | No |
| **5** | New diagnosis | *MYCN* amp., ALK R1275Q, ALK F1245L, ALK F1174L | *MYCN* amp. | **CHOP** | **4** | **Yes** | ALK R1275Q, ALK F1245L, ALK F1174L | Yes<br>ALK F1245L (1 of 2774 reads) |
| **6** | Relapsed | ALK R1275Q | ALK R1275Q | **FM** | **32** | | none | - |
| **7** | Relapsed | FLT3 D586G, PIK3CA H1047R | **ARID2 splice site 1716-1G>A** | **FM** | **57** | **Yes** | FLT3 D586G, PIK3CA H1047R | No |
| **8** | New diagnosis | none | none | **CHOP** | **1** | | none | - |
| **10** | Progressive disease | *MYCN* amp., *ALK* amp., ERBB2 G776C | *MYCN* amp., *ALK* amp., ERBB2 G776C, ***CHEK2* truncation exon 10, *ERBB4-ALMS1* rearrangement** | **FM** | **1** | | none | - |
| **11** | Relapsed | NF1 P2246fs*11 | **1L7R V253A,** TP53 A347T | **FM** | **21** | **Yes** | NF1 P2246fs*11 | No |
| **12** | Relapsed | none | **MLH1 E679*** | **FM** | **1** | | none | - |
| **13** | Relapsed | CDKN2A p14ARF Q57* | CDKN2A p14ARF Q57* | **FM** | **3** | | none | - |
| **16** | Relapsed | none | **ATR Q1108*** | **FM** | **38** | | none | - |
| **17** | Relapsed | none | **ASXL1 R774*** | **FM** | **56** | | none | - |
| **19** | Relapsed | *MYCN* amp., *ALK* amp. | *MYCN* amp., *ALK* amp. | **FM** | **4** | | none | - |
| **20** | Relapsed | none | none | **FM** | **0** | | none | - |
| **21** | Relapsed | none | none | **FM** | **5** | | none | - |
| **22** | Relapsed | BRCA2 E1773* | BRCA2 E1773* | **FM** | **0** | | none | - |
| **23** | Relapsed | ALK F1174I, TP53 R158C, *TERT* promoter -124C>T | ALK F1174I, TP53 R158C | **FM** | **0** | **Yes** | *TERT* promoter -124C>T | No |
| **24** | Relapsed | *MYCN* amp., *ALK* amp. | *MYCN* amp. *ALK* amp., ***CDKN2A/B* loss** | **FM** | **13** | | none | - |
| **31** | Relapsed | none | **ATRX G859fs*4** | **FM** | **11** | | none | - |
| **33** | Relapsed | PTPN11 E76G | none | **FM** | **0** | **Yes** | PTPN11 E76G | No |
| **34** | Relapsed | NF1 G2392*, CDKN2A splice site c.151-1 G>A | NF1 G2392*, ***CDKN2A/B* loss, ERBB4 R782P** | **FM** | **1** | **Yes** | CDKN2A splice site c.151-1 G>A | No |
| **38** | Relapsed | *MYCN* amp. | *MYCN* amp., **ARID1A N814fs*19**, **ASXL1 M1402fs*17**, ***CIC* loss**, **FANCA Q1307fs*2** | **FM** | **34** | | none | - |
| **39** | Relapsed | *MYCN* amp. | *MYCN* amp. | **FM** | **70** | | none | - |
| **41** | Relapsed | TP53 V157fs*13 | **ATRX E1447*, SDHA splice site 457-2_457delAGC** | **FM** | **0** | **Yes** | TP53 V157fs*13 | No |
| **42** | Relapsed | *MYCN* amp., ALK F1174L, ALK L1196M | *MYCN* amp., ALK F1174L | **FM** | **20** | **Yes** | ALK L1196M | No |
| **44** | Relapsed | *MYCN* amp., KIT D816V, NF1 splice site c.6643-1 G>C | *MYCN* amp., KIT D816V | **FM** | **2** | **Yes** | NF1 splice site c.6643-1 G>C | No |
| **47** | Relapsed | ALK R1275Q | ALK R1275Q | **FM** | **53** | | none | - |
| **49** | New diagnosis | none | none | **CHOP** | **10** | | none | - |

Amp., amplification; FM, Foundation Medicine FoundationOne® CDx assay; CHOP, Children's Hospital of Philadelphia NGS assay.

**Supplementary Table 6.** Summary of ctDNA identified genomic variants.

| Patient # | ctDNA identified variants (Bolded variants found in both ctDNA and tumor sequencing, variants in brackets represents data from standard clinical care ctDNA assays) | ctDNA identified variants (all/ctDNA unique) | ALK-RAS-MAPK variants (all/ctDNA unique) | DNA damage variants (all/ctDNA unique) | Targetable variants (all/ctDNA unique) | Potential therapy |
|---|---|---|---|---|---|---|
| 1 | TP53 V143A, BRCA2 E2301*, ***ERBB2* amp.**, ***MYCN* amp.** | 4/2 | 0/0 | 2/2 | 0/0 | - |
| 3 | TP53 E258D, **TP53 G244C**, TP53 T125M, TP53 G105C, [a]**ALK F1245V**, ***TERT* promoter -124C>T** | 6/3 | 1/0 | 4/3 | 1/0 | [a]ALKi |
| 5 | [a]ALK R1275Q, [a]ALK F1245L, [a]ALK F1174L, ***MYCN* amp.** | 4/3 | 3/3 | 0/0 | 3/3 | [a]ALKi |
| 6 | *ERBB2* amp., [a]**ALK R1275Q** | 2/1 | 1/0 | 0/0 | 1/0 | [a]ALKi |
| 7 | FLT3 D586G, [c]PIK3CA H1047R, TP53 P151H, [b]NRAS Q61K, TP53 E271G, TP53 P322fs*23, [c]PTEN D297fs*9, [d]*MET* amp., *BRAF* amp., [e]*CDKN2A-LDLRAD4* truncation | 10/10 | 2/2 | 3/3 | 5/5 | [b]MEKi, [c]PI3Ki, [d]METi, [e]CDK4/6i |
| 10 | [b]PTPN11 A72T, [a]**ALK F1174L, ERBB2 G776C**, ***MYCN* amp.**, [a]***ALK* amp.** | 5/1 | 3/1 | 0/0 | 3/1 | [a]ALKi, [b]MEKi |
| 11 | [b]NF1 P2246fs*11 | 1/1 | 1/1 | 0/0 | 1/1 | [b]MEKi |
| 13 | [b]PTPN11 G503E, BRCA2 I481fs*30, TP53 A161T, TP53 C176F, TP53 R280S, *ERBB2* amp., [d]***MET* amp.**, *BRAF* amp., [e]**CDKN2A p14ARF Q57*** | 9/7 | 2/2 | 4/4 | 3/1 | [b]MEKi, [d]METi, [e]CDK4/6i |
| 14 | **TP53 C135F**, [b]NF1 Y1369*, [b]NF1 G1699fs*11, [1]*ALK* rearrangement, ***MYCN* amp.** | 5/3 | 3/3 | 1/0 | 2/2 | [b]MEKi |
| 15 | ERRFI1 R247fs*16 | 1/1 | 0/0 | 0/0 | 0/0 | - |
| 16 | [b]*NF1* truncation | 1/1 | 1/1 | 0/0 | 1/1 | [b]MEKi |
| 18 | TP53 G279W, TP53 R248Q, *EZH2-TRIM24* truncation | 3/3 | 0/0 | 2/2 | 0/0 | - |
| 19 | [a]***ALK* amp.**, ***MYCN* amp.** | 2/0 | 1/0 | 0/0 | 1/0 | [a]ALKi |
| 21 | CDH1 P127fs*41, BRCA1 C1225*, ERRFI1 E108fs*7, *BRAF* amp., [1]*RAF1* rearrangement | 5/5 | 2/2 | 1/1 | 0/0 | - |
| 22 | **BRCA2 E1773*** | 1/0 | 0/0 | 1/0 | 0/0 | - |
| 23 | [a]**ALK F1174I, TP53 R158C**, *TERT* promoter -124C>T | 3/1 | 1/0 | 1/0 | 1/0 | [a]ALKi |
| 24 | [a]***ALK* amp.**, ***MYCN* amp.** | 2/0 | 1/0 | 0/0 | 1/0 | [a]ALKi |
| 25 | [a]**ALK F1245L** | 1/0 | 1/0 | 0/0 | 1/0 | [a]ALKi |
| 28 | ***MYCN* amp.**, ***TERT* promoter -146C>T**, [a]**ALK F1174L**, [a]***ALK* amp.**, [[a]ALK L1196M] | 5/1 | 3/1 | 0/0 | 3/1 | [a]ALKi |
| 30 | TP53 D281N | 1/1 | 0/0 | 1/1 | 0/0 | - |
| 32 | [b]NRAS Q61R, [a]ALK F1174I, [b]FGFR1 N546K, [b]NRAS Q61K, [b,f]BRAF V600E, [a]**ALK R1275Q** | 6/5 | 6/5 | 0/0 | 6/5 | [a]ALKi, [b]MEKi, [f]BRAFi |
| 33 | [b]PTPN11 E76G, [a]ALK R1275Q, ABL1 F317L, *ERBB2* amp. | 4/4 | 2/2 | 0/0 | 2/2 | [a]ALKi, [b]MEKi |
| 34 | [e]CDKN2A splice site c.151-1G>A, [b]**NF1 G2392*** | 2/1 | 1/0 | 0/0 | 2/1 | [b]MEKi, [e]CDK4/6i |
| 35 | [b,f]BRAF V600E, *ERBB2* amp., [a]**ALK R1275Q**, ***MYCN* amp.** | 4/2 | 2/1 | 0/0 | 2/1 | [a]ALKi, [b]MEKi, [f]BRAFi |
| 36 | [f]**BRAF G469A** | 1/0 | 1/0 | 0/0 | 1/0 | [f]BRAFi |
| 38 | TP53 R248Q, TP53 V218M, TP53 P177S, ***MYCN* amp.** | 4/3 | 0/0 | 3/3 | 0/0 | - |
| 39 | ***MYCN* amp.** | 1/0 | 0/0 | 0/0 | 0/0 | - |
| 41 | TP53 G334V, TP53 C277Y, TP53 V157fs*13 | 3/3 | 0/0 | 3/3 | 0/0 | - |
| 42 | [a]**ALK F1174L**, [a]**ALK L1196M**, ***MYCN* amp.**, [[e]CDKN2A p16INK4a R87L, [a]ALK R1275Q, [a]ALK F1245V, [a]ALK F1245L, [a]ALK F1174I, [b]NF1 S641fs*47, [b]NRAS Q61R, [e]CDKN2A p16INK4a E88* and P14ARF G102V] | 12/9 | 8/6 | 0/0 | 11/9 | [a]ALKi, [b]MEKi, [e]CDK4/6i |
| 43 | [b]FGFR1 N546K, [b]NRAS Q61R, [b,f]BRAF V600E, [b]NRAS Q61K, [a]ALK G1128A, [a]ALK L1196M, [a]**ALK R1275Q,** [ATM splice site c.5918+1G>A, ATM S614N, [a]ALK I1171N, [a]ALK G1202R, MTOR L1460P, [b]NRAS Q61L] | 13/12 | 10/9 | 0/0 | 10/9 | [a]ALKi, [b]MEKi, [f]BRAFi |
| 44 | [b]NF1 splice site c.6643-1 G>C, ***MYCN* amp., KIT D816V** | 3/1 | 1/1 | 0/0 | 1/1 | [b]MEKi |
| 45 | BRCA2 Y1655* | 1/1 | 0/0 | 1/1 | 0/0 | - |
| 46 | BRCA2 L638fs*9 | 1/1 | 0/0 | 1/1 | 0/0 | - |
| 47 | [a]**ALK R1275Q** | 1/0 | 1/0 | 0/0 | 1/0 | [a]ALKi |
| 48 | TP53 P98S, TP53 splice site c.375+1G>A | 2/2 | 0/0 | 2/2 | 0/0 | - |

[a]ALKi, ALK inhibition (11-16); [b]MEKi, MEK inhibition (16-24); [c]PI3Ki, PI3K inhibition (25-30); [d]METi, MET inhibition (31-33); [e]CDK4/6i, CDK4/6 inhibition (12,21,34-37); [f]BRAFi, BRAF inhibition (16). [1]Biological significance and potential clinical targetability of ALK and RAF1 rearrangements unclear. Amp, amplification. Patients 2,4,8,9,12,17, 20, 26, 27, 31, 37, and 49 had no ctDNA identified variants.

## Supplementary Figures

Supplementary Figure 1

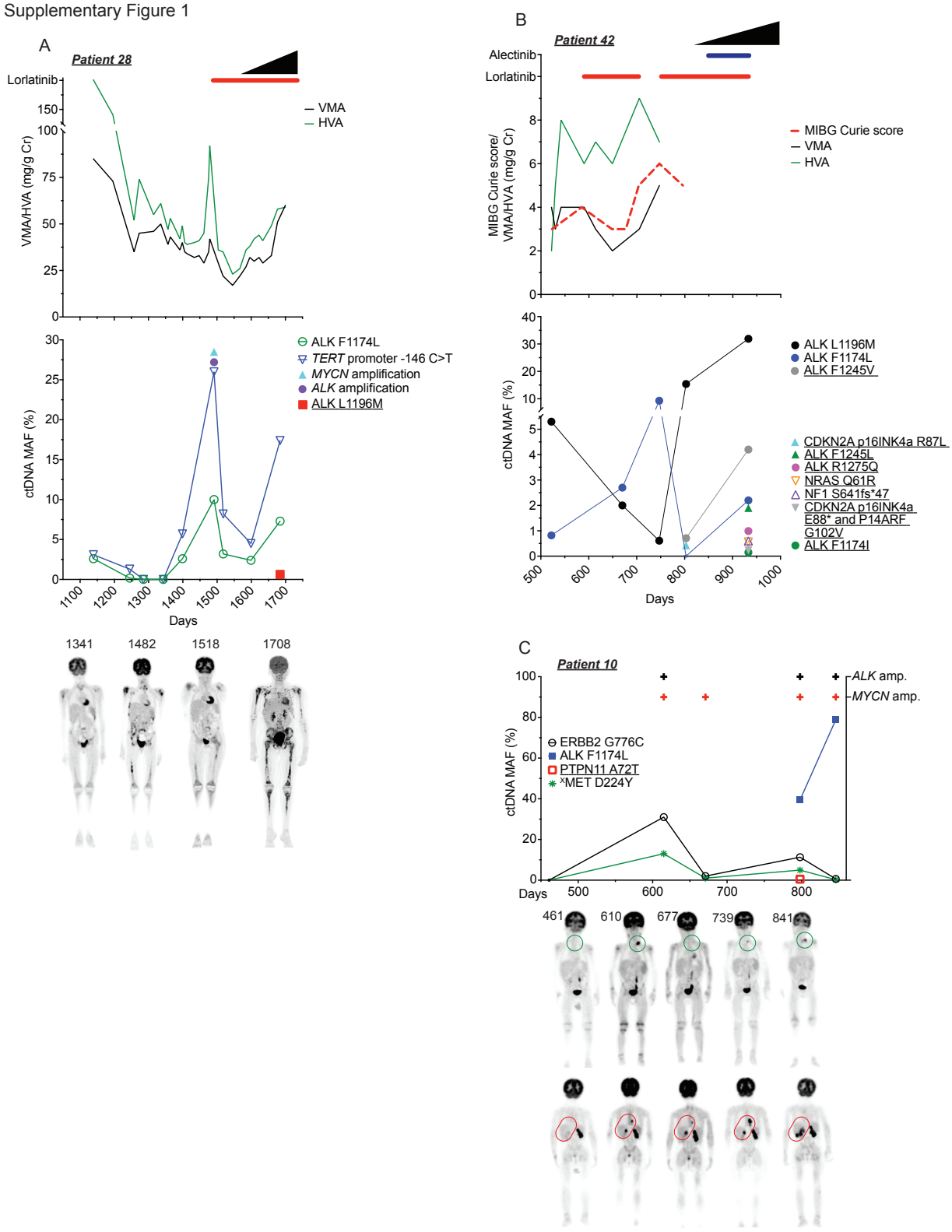

**Supplementary Figure 1. Serial profiling of ctDNA complements other disease surveillance approaches for patients with ALK-mutated neuroblastomas.**

(**A**) Serial ctDNA and clinical disease evaluation correlation plot for patient 28 showing relationship between VMA/HVA levels (top), ctDNA profiling data (middle), and representative coronal PET/CT and PET/MRI images (bottom, day of PET noted at top, day 1708 represents a PET/MRI vs. PET/CTs for the other time points). Black triangle and red line at top indicate approximate timing of clinical progression and lorlatinib treatment, respectively.

(**B**) Serial ctDNA and clinical disease evaluation correlation plot for patient 42 showing relationship between $^{123}$I-MIBG Curie scores and VMA/HVA levels (top) and ctDNA data (bottom). Black triangle, blue line, and red line at top indicate approximate timing of clinical progression (pathologic fracture and death), alectinib treatment, and lorlatinib treatment, respectively.

(**C**) Serial ctDNA and clinical disease evaluation correlation plot for patient 10 showing relationship between ctDNA data (top) and representative coronal PET images [bottom, day of PET noted at top of images; both anterior (top) and posterior (bottom) PET views shown]. The green circles on anterior PET images (top) identify the left neck tumor likely harboring an *ALK* amplification and an ERBB2 G776C variant, the size of which generally tracks with presence of those ctDNA variants in the blood. Conversely, the red circle in the posterior PET images (bottom) likely represent the tumor lesions that contain the ALK F1174L variant based on prior biopsy of this specific tumor showing an ALK F1174L variant and *MYCN* amplification. The ALK F1174L variant is identified in the blood when this specific tumor increases significantly in size (day 841). Underlined variants denote those unique to ctDNA. ctDNA samples 8 and 9 in **A** for patient 28 and 2-5 in **B** for patient 42 are from ctDNA profiling done as part of routine clinical care.

Supplementary Figure 2

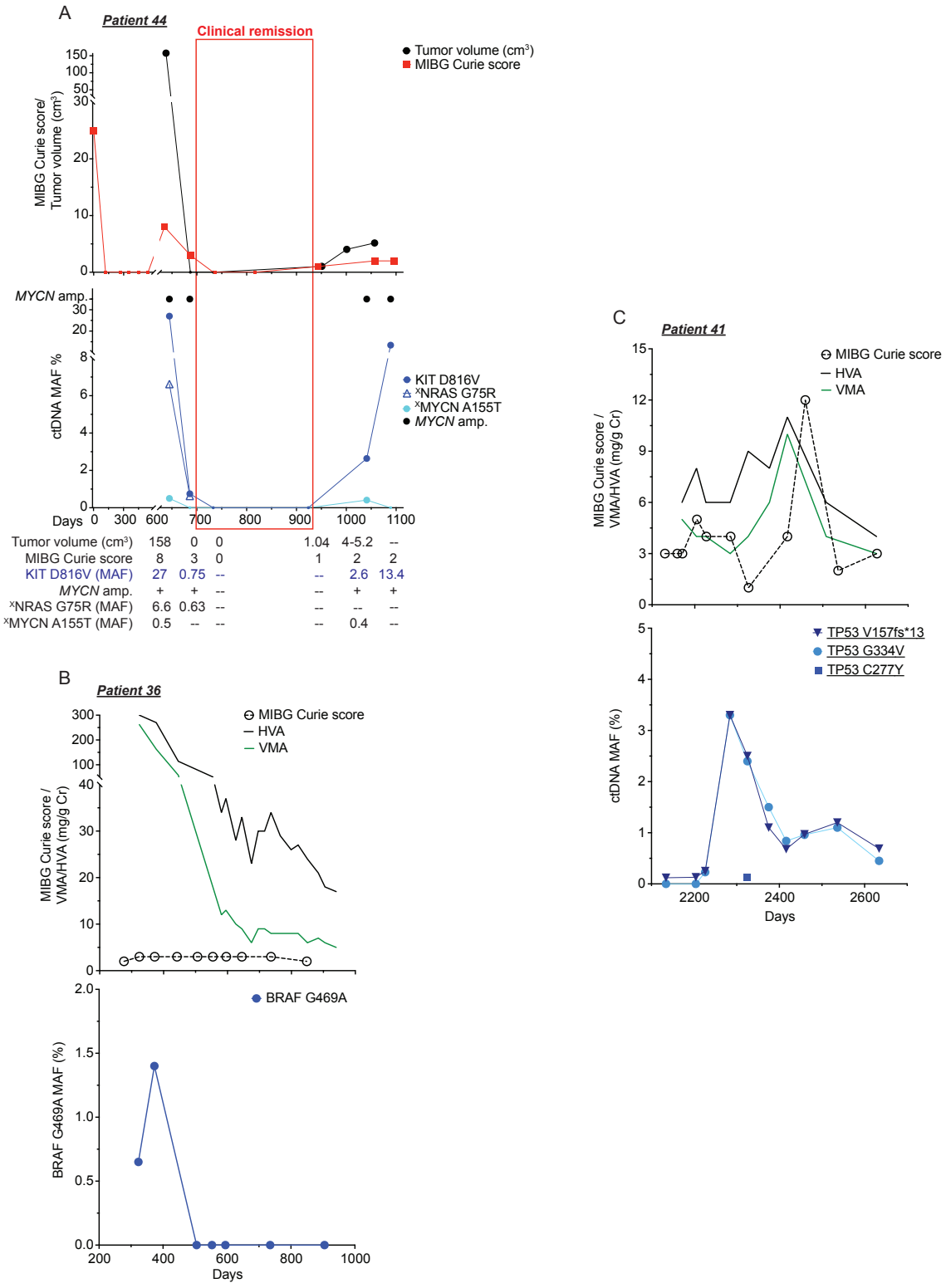

**Supplementary Figure 2. ctDNA profiling can augment standard disease surveillance practices in neuroblastoma.**

(**A**) Serial ctDNA and clinical disease evaluation correlation plot for patient 44 showing relationship between MRI tumor volumes and $^{123}$I-MIBG Curie scores (top) and ctDNA data (bottom). Clinical remission time frame denoted with red box. Imaging and ctDNA variant MAF summary shown in bottom table.

(**B**) Serial ctDNA and clinical disease evaluation correlation plot for patient 36 showing relationship between $^{123}$I-MIBG Curie scores and urine VMA/HVA levels (top) and BRAF G469A ctDNA MAFs (bottom).

(**C**) Serial ctDNA and clinical disease evaluation correlation plot for patient 41 showing limited correlation between $^{123}$I-MIBG Curie scores and urine VMA/HVA levels (top) and ctDNA data (bottom).

Amp, amplification. Underlined variants denote those unique to ctDNA and ($^{X}$) denotes variants of unknown significance (VUS).

Supplementary Figure 3

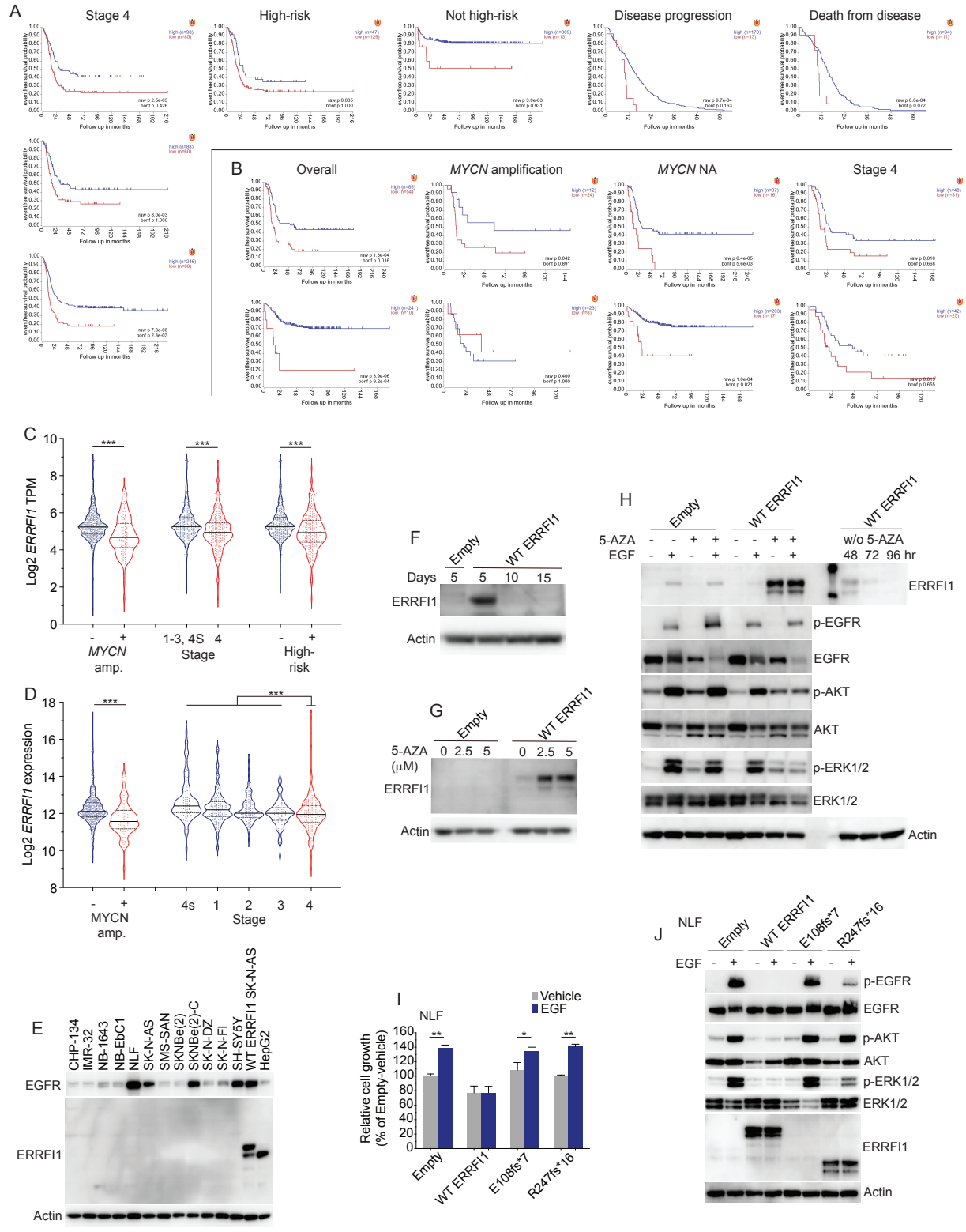

**Supplementary Figure 3. Low *ERRFI1* expression is associated with a clinically aggressive phenotype and a worse prognosis in neuroblastoma.**

(**A**) Neuroblastoma event-free survival (EFS) plots for patients with stage 4 tumors (left) or other clinical features as noted in 3 large neuroblastoma data sets, SEQC (n=498, top), Kocak (n=649; middle), and Cangelosi (n=786; bottom). EFS plots were generated in the Genomics Analysis and Visualization Platform (R2; https://hgserver1.amc.nl/cgi-bin/r2/main.cgi).

(**B**) Neuroblastoma event-free survival (EFS) plots for all patients (left), patients with *MYCN* amplified tumors (middle left), patients with *MYCN* non-amplified (NA) tumors (middle right), and for patients with stage 4 tumors (right) in 2 additional neuroblastoma data sets: Westermann, (n=144; top) and Oberthuer (n=251; bottom). EFS plots were generated in the Genomics Analysis and Visualization Platform (R2; https://hgserver1.amc.nl/cgi-bin/r2/main.cgi).

(**C, D**) *ERRFI1* expression in neuroblastoma tumors stratified by several clinical covariates (**C**; Westermann; n=579 and **D**; Kocak; n=649 data sets).

(**E**) ERRFI1 and EGFR western blot of neuroblastoma cell lines.

(**F**-**H**) Western blots of SK-N-AS ERRFI1 isogenic neuroblastoma cells over time (**F**), with and without 5-azacytidine treatment (**G**) and/or EGF treatment (**H**).

(**I**) Relative cell growth plots of the ERRFI1 isogenic NLF neuroblastoma cell lines after EGF stimulation (50 ng/mL).

(**J**) Western blot of the ERRFI1 isogenic NLF neuroblastoma cell lines after EGF stimulation (50 ng/mL).

*, $p<0.05$; **, $p<0.001$; ***, $p<0.0001$.

**Supplementary References**


1. Surrey LF, MacFarland SP, Chang F, Cao K, Rathi KS, Akgumus GT*, et al.* Clinical utility of custom-designed NGS panel testing in pediatric tumors. Genome Med **2019**;11(1):32 doi 10.1186/s13073-019-0644-8.
2. Surrey LF, Jain P, Zhang B, Straka J, Zhao X, Harding BN*, et al.* Genomic Analysis of Dysembryoplastic Neuroepithelial Tumor Spectrum Reveals a Diversity of Molecular Alterations Dysregulating the MAPK and PI3K/mTOR Pathways. J Neuropathol Exp Neurol **2019**;78(12):1100-11 doi 10.1093/jnen/nlz101.
3. Jain P, Surrey LF, Straka J, Luo M, Lin F, Harding B*, et al.* Novel FGFR2-INA fusion identified in two low-grade mixed neuronal-glial tumors drives oncogenesis via MAPK and PI3K/mTOR pathway activation. Acta Neuropathol **2018**;136(1):167-9 doi 10.1007/s00401-018-1864-5.
4. Zhang W, Yu Y, Hertwig F, Thierry-Mieg J, Thierry-Mieg D, Wang J*, et al.* Comparison of RNA-seq and microarray-based models for clinical endpoint prediction. Genome Biol **2015**;16:133 doi 10.1186/s13059-015-0694-1 10.1186/s13059-015-0694-1 [pii].
5. Kocak H, Ackermann S, Hero B, Kahlert Y, Oberthuer A, Juraeva D*, et al.* Hox-C9 activates the intrinsic pathway of apoptosis and is associated with spontaneous regression in neuroblastoma. Cell Death Dis **2013**;4:e586 doi cddis201384 [pii] 10.1038/cddis.2013.84.
6. Hartlieb SA, Sieverling L, Nadler-Holly M, Ziehm M, Toprak UH, Herrmann C*, et al.* Alternative lengthening of telomeres in childhood neuroblastoma from genome to proteome. Nat Commun **2021**;12(1):1269 doi 10.1038/s41467-021-21247-8.
7. Cangelosi D, Morini M, Zanardi N, Sementa AR, Muselli M, Conte M*, et al.* Hypoxia Predicts Poor Prognosis in Neuroblastoma Patients and Associates with Biological

Mechanisms Involved in Telomerase Activation and Tumor Microenvironment Reprogramming. Cancers (Basel) **2020**;12(9) doi 10.3390/cancers12092343.

8. Oberthuer A, Berthold F, Warnat P, Hero B, Kahlert Y, Spitz R*, et al.* Customized oligonucleotide microarray gene expression-based classification of neuroblastoma patients outperforms current clinical risk stratification. J Clin Oncol **2006**;24(31):5070-8 doi 10.1200/JCO.2006.06.1879.
9. Koche RP, Rodriguez-Fos E, Helmsauer K, Burkert M, MacArthur IC, Maag J*, et al.* Extrachromosomal circular DNA drives oncogenic genome remodeling in neuroblastoma. Nat Genet **2020**;52(1):29-34 doi 10.1038/s41588-019-0547-z.
10. Helmsauer K, Valieva ME, Ali S, Chamorro Gonzalez R, Schopflin R, Roefzaad C*, et al.* Enhancer hijacking determines extrachromosomal circular MYCN amplicon architecture in neuroblastoma. Nat Commun **2020**;11(1):5823 doi 10.1038/s41467-020-19452-y.
11. Foster JH, Voss SD, Hall DC, Minard CG, Balis FM, Wilner K*, et al.* Activity of Crizotinib in Patients with ALK-Aberrant Relapsed/Refractory Neuroblastoma: A Children's Oncology Group Study (ADVL0912). Clin Cancer Res **2021**;27(13):3543-8 doi 10.1158/1078-0432.CCR-20-4224.
12. Wood AC, Krytska K, Ryles HT, Infarinato NR, Sano R, Hansel TD*, et al.* Dual ALK and CDK4/6 Inhibition Demonstrates Synergy against Neuroblastoma. Clin Cancer Res **2017**;23(11):2856-68 doi 10.1158/1078-0432.CCR-16-1114.
13. Krytska K, Ryles HT, Sano R, Raman P, Infarinato NR, Hansel TD*, et al.* Crizotinib Synergizes with Chemotherapy in Preclinical Models of Neuroblastoma. Clin Cancer Res **2016**;22(4):948-60 doi 10.1158/1078-0432.CCR-15-0379.
14. Infarinato NR, Park JH, Krytska K, Ryles HT, Sano R, Szigety KM*, et al.* The ALK/ROS1 Inhibitor PF-06463922 Overcomes Primary Resistance to Crizotinib in ALK-Driven Neuroblastoma. Cancer Discov **2016**;6(1):96-107 doi 10.1158/2159-8290.CD-15-1056.

15. Bresler SC, Weiser DA, Huwe PJ, Park JH, Krytska K, Ryles H*, et al.* ALK mutations confer differential oncogenic activation and sensitivity to ALK inhibition therapy in neuroblastoma. Cancer Cell **2014**;26(5):682-94 doi 10.1016/j.ccell.2014.09.019.
16. Mlakar V, Morel E, Mlakar SJ, Ansari M, Gumy-Pause F. A review of the biological and clinical implications of RAS-MAPK pathway alterations in neuroblastoma. J Exp Clin Cancer Res **2021**;40(1):189 doi 10.1186/s13046-021-01967-x.
17. Tomida A, Yagyu S, Nakamura K, Kubo H, Yamashima K, Nakazawa Y*, et al.* Inhibition of MEK pathway enhances the antitumor efficacy of chimeric antigen receptor T cells against neuroblastoma. Cancer Sci **2021**;112(10):4026-36 doi 10.1111/cas.15074.
18. Takemoto M, Tanaka T, Tsuji R, Togashi Y, Higashi M, Fumino S*, et al.* The synergistic antitumor effect of combination therapy with a MEK inhibitor and YAP inhibitor on pERK-positive neuroblastoma. Biochem Biophys Res Commun **2021**;570:41-6 doi 10.1016/j.bbrc.2021.07.028.
19. Healy JR, Hart LS, Shazad AL, Gagliardi ME, Tsang M, Elias J*, et al.* Limited antitumor activity of combined BET and MEK inhibition in neuroblastoma. Pediatr Blood Cancer **2020**;67(6):e28267 doi 10.1002/pbc.28267.
20. Xu DQ, Toyoda H, Qi L, Morimoto M, Hanaki R, Iwamoto S*, et al.* Induction of MEK/ERK activity by AZD8055 confers acquired resistance in neuroblastoma. Biochem Biophys Res Commun **2018**;499(3):425-32 doi 10.1016/j.bbrc.2018.03.143.
21. Hart LS, Rader J, Raman P, Batra V, Russell MR, Tsang M*, et al.* Preclinical Therapeutic Synergy of MEK1/2 and CDK4/6 Inhibition in Neuroblastoma. Clin Cancer Res **2017**;23(7):1785-96 doi 10.1158/1078-0432.CCR-16-1131.
22. Woodfield SE, Zhang L, Scorsone KA, Liu Y, Zage PE. Binimetinib inhibits MEK and is effective against neuroblastoma tumor cells with low NF1 expression. BMC Cancer **2016**;16:172 doi 10.1186/s12885-016-2199-z.

23. Tanaka T, Higashi M, Kimura K, Wakao J, Fumino S, Iehara T*, et al.* MEK inhibitors as a novel therapy for neuroblastoma: Their in vitro effects and predicting their efficacy. J Pediatr Surg **2016**;51(12):2074-9 doi 10.1016/j.jpedsurg.2016.09.043.

24. Eleveld TF, Oldridge DA, Bernard V, Koster J, Colmet Daage L, Diskin SJ*, et al.* Relapsed neuroblastomas show frequent RAS-MAPK pathway mutations. Nat Genet **2015**;47(8):864-71 doi 10.1038/ng.3333.

25. Chilamakuri R, Agarwal S. Dual Targeting of PI3K and HDAC by CUDC-907 Inhibits Pediatric Neuroblastoma Growth. Cancers (Basel) **2022**;14(4) doi 10.3390/cancers14041067.

26. Holzhauser S, Lukoseviciute M, Papachristofi C, Vasilopoulou C, Herold N, Wickstrom M*, et al.* Effects of PI3K and FGFR inhibitors alone and in combination, and with/without cytostatics in childhood neuroblastoma cell lines. Int J Oncol **2021**;58(2):211-25 doi 10.3892/ijo.2021.5167.

27. Mohlin S, Hansson K, Radke K, Martinez S, Blanco-Aparicio C, Garcia-Ruiz C*, et al.* Anti-tumor effects of PIM/PI3K/mTOR triple kinase inhibitor IBL-302 in neuroblastoma. EMBO Mol Med **2020**;12(1):e11749 doi 10.15252/emmm.201911749.

28. Subramonian D, Phanhthilath N, Rinehardt H, Flynn S, Huo Y, Zhang J*, et al.* Regorafenib is effective against neuroblastoma in vitro and in vivo and inhibits the RAS/MAPK, PI3K/Akt/mTOR and Fos/Jun pathways. Br J Cancer **2020**;123(4):568-79 doi 10.1038/s41416-020-0905-8.

29. Wong RLY, Wong MRE, Kuick CH, Saffari SE, Wong MK, Tan SH*, et al.* Integrated Genomic Profiling and Drug Screening of Patient-Derived Cultures Identifies Individualized Copy Number-Dependent Susceptibilities Involving PI3K Pathway and 17q Genes in Neuroblastoma. Front Oncol **2021**;11:709525 doi 10.3389/fonc.2021.709525.

30. Yu X, Fan H, Jiang X, Zheng W, Yang Y, Jin M*, et al.* Apatinib induces apoptosis and autophagy via the PI3K/AKT/mTOR and MAPK/ERK signaling pathways in neuroblastoma. Oncol Lett **2020**;20(4):52 doi 10.3892/ol.2020.11913.

31. Daudigeos-Dubus E, Le Dret L, Bawa O, Opolon P, Vievard A, Villa I*, et al.* Dual inhibition using cabozantinib overcomes HGF/MET signaling mediated resistance to pan-VEGFR inhibition in orthotopic and metastatic neuroblastoma tumors. Int J Oncol **2017**;50(1):203-11 doi 10.3892/ijo.2016.3792.

32. Crosswell HE, Dasgupta A, Alvarado CS, Watt T, Christensen JG, De P*, et al.* PHA665752, a small-molecule inhibitor of c-Met, inhibits hepatocyte growth factor-stimulated migration and proliferation of c-Met-positive neuroblastoma cells. BMC Cancer **2009**;9:411 doi 10.1186/1471-2407-9-411.

33. Hecht M, Schulte JH, Eggert A, Wilting J, Schweigerer L. The neurotrophin receptor TrkB cooperates with c-Met in enhancing neuroblastoma invasiveness. Carcinogenesis **2005**;26(12):2105-15 doi 10.1093/carcin/bgi192.

34. Geoerger B, Bourdeaut F, DuBois SG, Fischer M, Geller JI, Gottardo NG*, et al.* A Phase I Study of the CDK4/6 Inhibitor Ribociclib (LEE011) in Pediatric Patients with Malignant Rhabdoid Tumors, Neuroblastoma, and Other Solid Tumors. Clin Cancer Res **2017**;23(10):2433-41 doi 10.1158/1078-0432.CCR-16-2898.

35. Rihani A, Vandesompele J, Speleman F, Van Maerken T. Inhibition of CDK4/6 as a novel therapeutic option for neuroblastoma. Cancer Cell Int **2015**;15:76 doi 10.1186/s12935-015-0224-y.

36. Rader J, Russell MR, Hart LS, Nakazawa MS, Belcastro LT, Martinez D*, et al.* Dual CDK4/CDK6 inhibition induces cell-cycle arrest and senescence in neuroblastoma. Clin Cancer Res **2013**;19(22):6173-82 doi 10.1158/1078-0432.CCR-13-1675.

37. Gogolin S, Ehemann V, Becker G, Brueckner LM, Dreidax D, Bannert S*, et al.* CDK4 inhibition restores G(1)-S arrest in MYCN-amplified neuroblastoma cells in the context of

doxorubicin-induced DNA damage. Cell Cycle **2013**;12(7):1091-104 doi 10.4161/cc.24091.